

A PROPOSED MULTIFUNCTIONAL MULTICHANNEL RECEIVER FOR SGSLR

J.J. Degnan¹ and R. L. Machan²

, Sigma Space Corporation, 4600 Forbes Blvd., Lanham, MD, 20760 USA,

¹john.degnan@sigmaspace.com, ²roman.machan@sigmaspace.com

1.0 INTRODUCTION

In the present paper, we describe a device proposed for possible use in SGSLR which, when combined with a segmented anode photomultiplier or other detector array, performs multiple functions as: (1) a multichannel Event Timer (ET) with extremely low deadtime (<2 nsec) per channel; (2) an automated pointing error correction system which monitors and reports the angular offset between the receiver optical axis and the target satellite; and (3) an “Electronic Spatial Filter” which eliminates the vast majority of noise counts which do not emanate from the immediate angular vicinity of the satellite. The device design draws heavily from Sigma’s multibeam 3D imaging lidar experience and is relatively indifferent to sensitivity or gain non-uniformities in the array detector which complicated an earlier approach based on balancing the outputs of a quadrant detector [1]. A block diagram of the legacy SLR2000/NGSLR approach to automated pointing correction is illustrated in Figure 1.

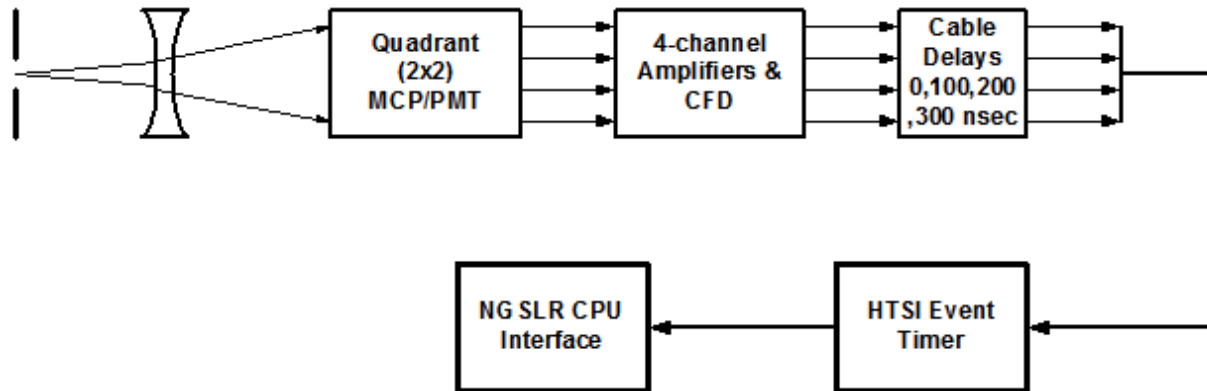


Figure 1. Block diagram of legacy SLR2000/NGSLR quadrant detector approach to automated pointing correction.

In the quadrant approach, solar and satellite returns collected by the telescope pass through the spatial filter. A negative lens diverges the light so that it fills most of the Quadrant MCP/PMT Photocathode. Each quadrant generates an electrical pulse for each detected photon (signal or noise). The electrical pulses from each quadrant are amplified independently to fall within the desired voltage range for the Constant Fraction Discriminator (CFD) for maximum range stability. Independent amplification also helps compensate for any gain nonuniformity in the MCP/PMT which might result in a false pointing error. The outputs from each quadrant are delayed by multiples of 100 nanoseconds so that their arrival times can be recorded by the HTSI Event Timer (ET), which has a 60 nsec recovery time following a photon event. On average, solar noise counts are distributed uniformly among the four quadrants. Satellite returns centered

on the quadrant are also distributed uniformly among the quadrants unless the telescope is not pointed directly at the satellite. Thus, an imbalance in counts among the four quadrants, as measured over a short period of time, allows the computation of the magnitude and direction of the pointing error. This information is then used to drive the telescope/tracking gimbal mount and correct the pointing error and remove the imbalance.

While valid in concept, we were unable to implement this approach successfully for a number of reasons:

1. Poor alignment of the off-axis telescope and tracking mount purchased from two different vendors resulted in a large (20 arcsec), amorphous (i.e. non-circular) star image quality in the focal plane making quadrant balancing difficult, if not impossible.
2. The photocathode sensitivity and microchannel plate gain can have a fair amount of variation further complicating balancing of the quadrants.
3. All of the noise photons detected are passed on to the receiver and, since they are distributed uniformly over the range gate, can affect the measured return normal point centroid for HEO satellites with low signal count rates.

2.0 PROPOSED MULTIPURPOSE MULTICHANNEL RECEIVER

A block diagram of our proposed receiver is illustrated in Figure 1. Solar and satellite returns collected by the telescope pass through the spatial filter (assumed to be a circular iris so it can be easily varied for day vs night operations). A telephoto lens reimages the spatial filter/iris onto the photocathode of a $N \times N$ ($N \leq 10$) Segmented Anode MCP/PMT. For the purposes of this discussion, we will assume $N = 10$ since this is our standard lidar configuration and provides good angular resolution. Each of the pixels within the iris FOV generates an electrical pulse for each detected photon (signal or noise). The electrical pulses from each pixel are then amplified to ensure that a single photon return will generate a voltage in excess of the required comparator threshold.

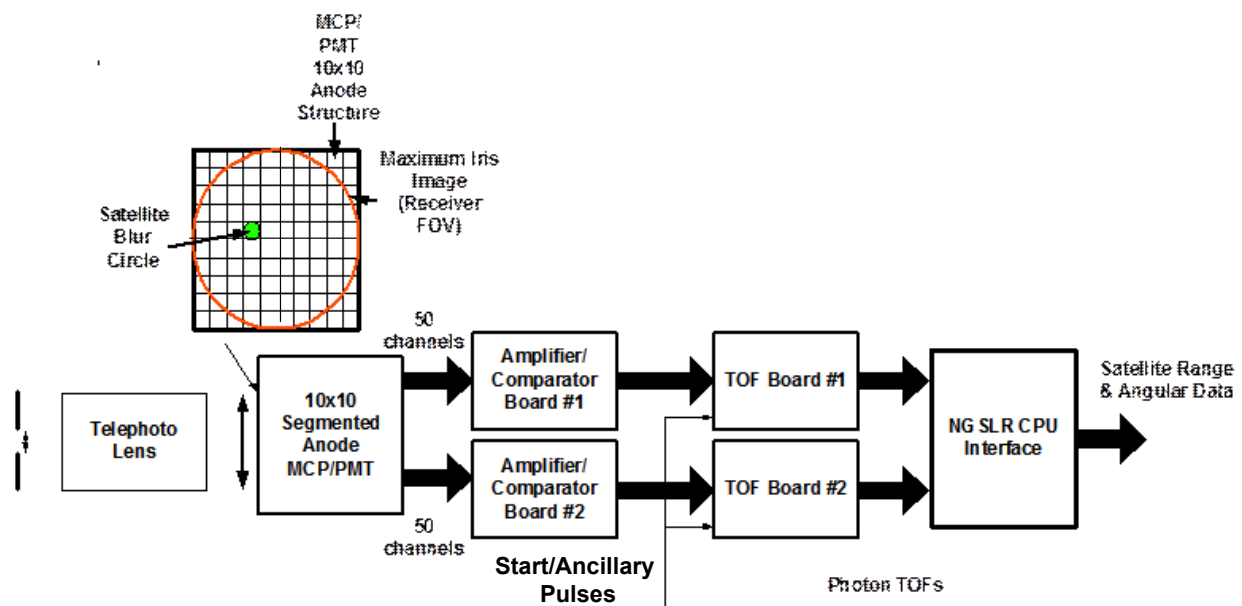


Figure 2: Block diagram of the proposed multichannel pointing correction system.

The current Time-of-Flight (TOF) boards in our 3D imaging lidars time-tag each photon event with an RMS precision of ± 23 picoseconds (3.4 mm RMS) and a pixel recovery time of less than 2 nanoseconds between photon events. Automated calibration provides real-time updates of timer delays as affected by voltage and temperature.

On average, solar noise counts will be distributed uniformly among the 88 pixels, within the iris FOV, while satellite returns will be concentrated on a small number of pixels determined by the image size at the MCP/PMT. Thus, the pixel with the most counts (dark green pixel in Figure 3) determines the angular position of the satellite relative to the receiver axis centered on the array detector. In the event that the satellite image spills over into adjacent pixels, inclusion of the 8 nearest pixels in a centroid computation may be useful in better defining the satellite angular position. The magnitude and direction of the pointing error would be transmitted to the SGSLR interface to drive the telescope/tracking gimbal mount and correct for the pointing error.

Since they are spatially uncorrelated with the satellite, the counts in the remaining 79 pixels located within the iris (red circle) can be discounted as noise, thereby reducing the number of noise counts by $79/88 = 90\%$ and greatly reducing the potential for noise induced range bias errors in weak links [3]. Furthermore, the 12 unused timing channels outside the red circle (3 at each corner) can be allocated to record other important timing events (e.g. start pulse, GPS 1pps, MOBLAS synch, etc.). The current 100 channel lidars use two amplifiers and two Time-of-Flight (TOF) cards, but reducing the size of the $N \times N$ array to $N \leq 7$ would require only one card, halving the production cost for multiple systems. Odd N has the additional advantage that, for perfect pointing, the receive optical axis falls on one central pixel whereas for even N the receive optical axis would fall between 4 pixels. For all values of N , the three corner pixels are still available for ancillary timing signals. The total array FOV should not exceed the divergence of the transmit beam since the outer pixels would be unable to record signal counts anyway. This implies, for example, that the angular FOV of each pixel for $N=5$ would be twice that of an $N=10$ pixel.

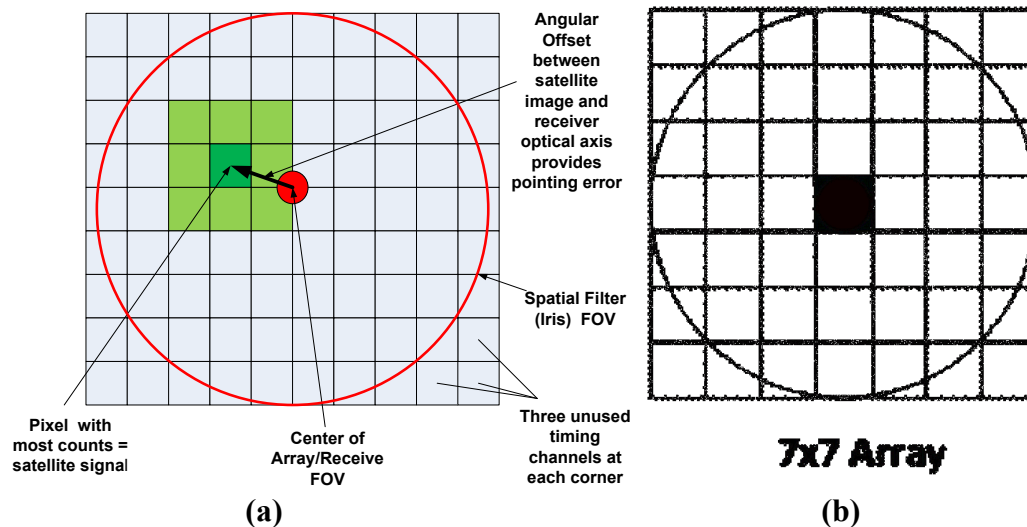


Figure 3: (a) Closeup view of a 10x10 anode array. (b) 7x7 array with center pixel illuminated under conditions of perfect pointing.

Figure 4 provides a block diagram of the proposed multichannel timing receiver. It is based on a 3rd generation, flight proven Sigma design with excellent performance and is therefore very low risk. It is equipped with high speed, high bandwidth interconnects, and automated calibration provides real-time updates of timer delays as affected by voltage and temperature. It is also highly flexible, since the SGSLR Linux computer would send commands to define key parameters such as # of laser shots in an integration frame, mode (diagnostic, functional), gate width/position, start/stop collecting, etc and take independent actions based on the results fed back to it. Except for the Data Processing FPGAs, the proposed receiver is identical to that used in Sigma's line of single photon sensitive 3D Imaging Lidars. Photos of the actual amplifier and Time-of-Flight (TOF) boards are provided in Figure 5.

Multifunctional Range Receiver

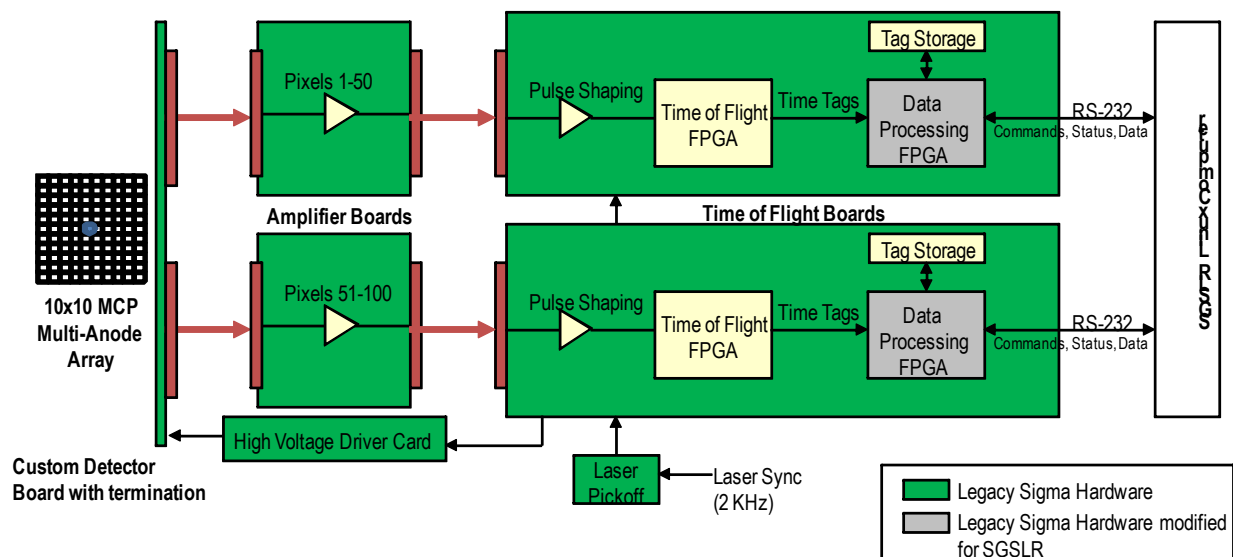


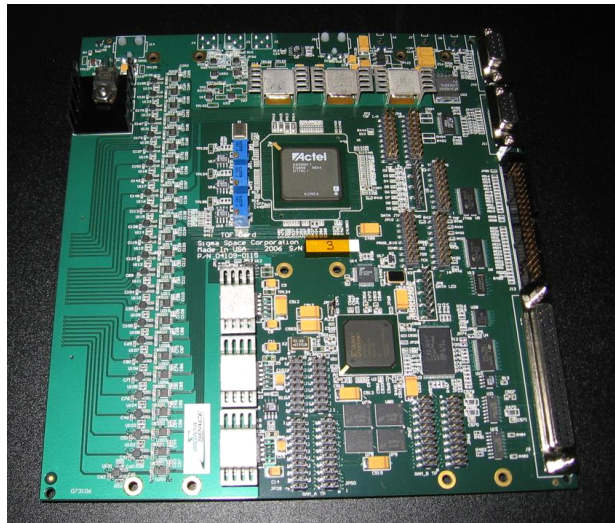
Figure 4: Block diagram of the proposed multichannel timing receiver

3.0 SUMMARY

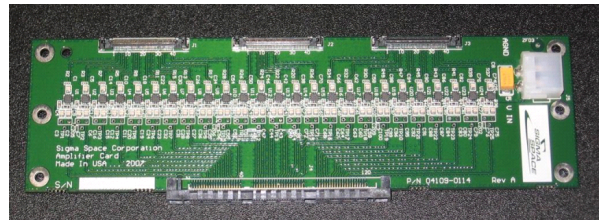
The proposed system provides an accurate measure of the magnitude and direction of the angular error between the satellite and the receiver optical axis while simultaneously serving as a Multichannel Event Timer, providing up to 100 channels of multistop ranging data having deadtimes less than 2 nsec. The current unmodified range receiver used in our 3D imaging lidars has an RMS timing accuracy of 23 psec (3.4 mm range RMS). With the exception of the new SGSLR interface, all of the required components have been successfully demonstrated in Sigma's single photon sensitive 3D imaging lidars at laser repetition rates up to 32 kHz.

Enhanced timer resolutions down to 1.8 psec (0.3 mm) can be achieved with deadtimes less than 3.4 ns with the same hardware through the use of multiple (2 to 4) timing channels per pixel. However, this modification would require firmware updates to the programmable TOF FPGAs in Figure 4. Furthermore, such enhancements may not be warranted in the presence of larger

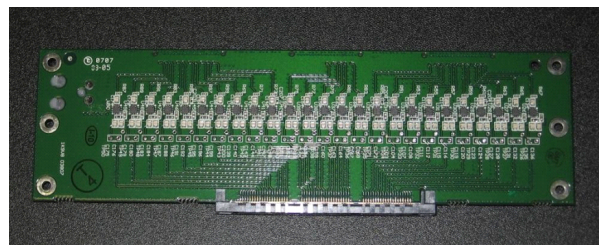
sources of range error, such as laser pulsewidth, detector impulse response, and satellite signature effects. Also, under our inhouse lidar program, Sigma is currently exploring possible alternatives to Segmented Anode MCP/PMTs which may have flexibility, cost, availability, and lifetime advantages. All of these detector/receiver options will be explored in our trade study.



TOF Card – Top Side



Amplifier Card – Top Side



Amplifier Card – Bottom Side

Figure 5: Photos of the existing amplifier and TOF cards used in Sigma’s Imaging Lidars.

Although modest image blur in the iris is still a requirement, the proposed receiver is significantly less sensitive to nonuniformities in detector sensitivity or gain and has the additional ability to eliminate the vast majority of noise counts within the receiver FOV that do not originate in the angular vicinity of the satellite being tracked. For the 10x10 example shown, this eliminates about 90% of the noise that can bias the satellite centroid range measurement in sufficiently weak HEO passes. Currently, the noise counts are reduced by HTSI in post-processing [3].

4.0 REFERENCES

- [1] J. Degnan, J. McGarry, SLR2000: Eyesafe and autonomous satellite laser ranging at kilohertz rates, Laser Radar Ranging and Atmospheric Lidar Techniques, pp. 63-77, London, UK, Sept. 24-26 SPIE 3218, 63-77 (1997).
- [2] J. Degnan, C. Field, Moderate to High Altitude, Single Photon Sensitive, 3D Imaging Lidars”, SPIE Defense Sensing Symposium, SPIE 9114-16, Baltimore, MD, May 5-9, 2014.
- [3] C. Clarke, J. Degnan, J. McGarry, J. Horvath, Background Noise Suppression for Increased Data Acceptance, 19th International Workshop on Laser Ranging, 3277, Annapolis, Maryland, October 2014, <<http://cddis.gsfc.nasa.gov/lw19/>>